Numerical Prediction of Liquid-Solid Turbulent Flows on Moving Boundaries with ALE Method

Satoru Ushijima
Dept. of Global Environment Engineering, Kyoto University
Kyoto, 606-8501, Japan
ushijima@gee.kyoto-u.ac.jp

Iehisa Nezu
Dept. of Global Environment Engineering, Kyoto University
Kyoto, 606-8501, Japan
nezu@nezu.gee.kyoto-u.ac.jp

ABSTRACT

A computational method has been proposed to predict liquid-solid turbulent flows on moving bottom boundaries. The two-phase flows are numerically predicted with a two-equation turbulence model which is derived from a liquid-solid two-fluid model. This numerical model includes an algebraic equation for the turbulence energy in a dispersed phase as well as the transport equations for turbulence energy and its dissipation rate in a liquid phase.

The profiles of the bottom boundaries are represented with curvilinear coordinates. The coordinates are regenerated at the appointed time steps to respond to the unsteady deformation of the boundaries, while the internal grid points are rearranged on the basis of the arbitrary Lagrangian-Eulerian (ALE) formulation. Accordingly, the interaction between the two-phase flows and the deformation of boundary shapes is reasonably taken into account in the present method.

This computational method was applied to the deformation of the sand bed profiles caused by horizontal turbulent jet flows. As a result, it was shown that the predicted bed profile on the center line, including the deeply scoured area, is in good agreement with the measurements.

INTRODUCTION

The accurate estimation for the sand bed profiles deformed by turbulent flows is important in various civil engineering problems, since it is closely related to the long-term stability of the hydraulic structures. Typical examples can be found in the local scour on river beds around bridge piers and sand bed deformation in front of power stations when cooling-water is discharged with high velocity from their submerged outlets. In these problems, three-dimensional flow field, including some amount of sands, should be treated as liquid-solid two-phase flows and the bottom boundaries consisting of sand particles can be recognized as moving boundaries due to their unsteady and nonuniform deformation.

In this paper, a computational method has been proposed to predict liquid-solid turbulent flows on moving boundaries. The flow field is numerically simulated with a turbulence model, which has been derived from the governing equations for a liquid-solid two-fluid model. The present numerical model consists of continuity and momentum equations for both liquid and solid phases together with the transport equations for turbulence energy and its dissipation rate in a liquid phase. In addition, an algebraic equation is utilized to accurately predict turbulence energy in a dispersed phase.

The deformation of the boundary profiles is estimated with the predicted concentration flux of solid particles. The complicated-shaped boundary profiles are represented with the three-dimensional curvilinear coordinates (Thompson et al. 1985), which are regenerated at suitable intervals to respond to the unsteady deformation. The grid treatment is based on the arbitrary Lagrangian-Eulerian (ALE) formulation (Hirt et al. 1974), which is one of the most effective methods to deal with moving boundaries. The computations of the liquid-solid flows and the deformation of boundary profiles are performed alternately with different computational time increments in order to take account of the mutual interaction as well as the computational efficiency (Ushijima 1996).

This computational method has been applied to local scouring of a sand bed caused by the cooling-water discharge from a power station. Through the comparison with the field measurements, the validity of the prediction method is discussed.

NUMERICAL MODELING

Two-Fluid Turbulence Model

The governing equations are based on a liquid-solid two-fluid model, in which the continuity and momentum equations are derived for both liquid and solid phases (Murray 1965). A two-equation turbulence model can be obtained from the two-fluid model assuming that the instantaneous values in liquid-solid flows are separated into time- or ensemble-average and fluctuating quantities as done in the derivation of usual turbulence models. Thus, the velocity components in the liquid and solid phases, bearing subscripts f and p respectively in this paper, are written as $u_{fi} = U_{fi} + u'_{fi}$ and $u_{pi} = U_{pi} + u'_{pi}$, where capital and 'single-prime' letters stand for the average and fluctuating components respectively. Similarly, pressure p in the liquid phase and the volumetric concentration of the solid phase c are given by $p = P + p'$ and $c = C + c'$ respectively.

Since the volumetric concentration c is sufficiently small in this paper, the following relationship is established for the liquid phase fraction in a unit volume, ϕ $(= 1 - c)$, as done by Hosoda (Hosoda and Yogoshi 1987):

$$\frac{1}{\phi} = \frac{1}{1-C-c'} \approx \frac{1}{1-C} + \frac{c'}{(1-C)^2} \equiv \frac{1}{\Phi} + \frac{1}{\phi'} \qquad (1)$$

In addition, the second term on the right hand side of Eq.(1) is generally much smaller than the first term. Thus, the Eq.(1) is only applied to the external force and liquid-solid interactive force in which the evaluation of volumetric concentration is relatively important. In contrast, the following relationship is utilized for the rest of the terms in all governing equations:

$$\frac{1}{\phi} \approx \frac{1}{1-C} = \frac{1}{\Phi} \qquad (2)$$

With the above relationships for instantaneous values the following continuity equations can be derived for the liquid and solid phases:

$$\frac{\partial \Phi}{\partial t} + \frac{\partial}{\partial x_i}(\Phi U_{fi}) = 0 \qquad (3)$$

$$\frac{\partial C}{\partial t} + \frac{\partial}{\partial x_i}\left(C U_{pi} + \overline{c' u'_{pi}}\right) = 0 \qquad (4)$$

where the densities ρ_f and ρ_p in both phases are taken as constant.

In addition, the momentum equations are obtained for the averaged components as

$$\frac{D_f U_{fi}}{Dt} = \frac{1}{\Phi}F_i - \frac{1}{\Phi}\frac{1}{\rho_f}\frac{\partial P}{\partial x_i} - \frac{1}{\Phi}\frac{\partial}{\partial x_j}\left(\Phi \overline{u'_{fi} u'_{fj}}\right) + \nu_f \frac{\partial^2 U_{fi}}{\partial x_j^2} - \frac{18\nu_f}{d^2}\frac{1}{1-C}\left[C\left(U_{fi} - U_{pi}\right) + \overline{c' u'_{fi}} - \overline{c' u'_{pi}}\right] \qquad (5)$$

$$\frac{D_p U_{pi}}{Dt} = \left(1 - \frac{\rho_f}{\rho_p}\right)F_i - \frac{1}{C}\frac{\partial}{\partial x_j}\left(C\overline{u'_{pi} u'_{pj}}\right) + \nu_p \frac{\partial^2 U_{pi}}{\partial x_j^2} + \frac{18\nu_f}{d^2}\frac{\rho_f}{\rho_p}\left(U_{fi} - U_{pi}\right) \qquad (6)$$

where F_i is external force, ν_f and ν_p are kinematic viscosities and d is the representative diameter of a solid particle. In the momentum equations, the liquid-solid interactive force is given by the Stokes law. The Lagrangian differential operators in Eqs.(5) and (6) are given by

$$\frac{D_X}{Dt} = \frac{\partial}{\partial t} + \left(U_{Xj} - U_{0j}\right)\frac{\partial}{\partial x_j} \qquad (7)$$

where subscript X means the phase (X takes f or p) and U_{0j} corresponds to the grid velocity which arises in the grid regeneration based on the ALE method.

The transport equation for the turbulence energy k_f in a liquid phase can be derived from the equation of u'_{fi} as

$$\frac{D_f k_f}{Dt} = P_{kf} + \frac{\overline{c' u'_{fi}}}{(1-C)^2}F_i + \frac{\partial}{\partial x_j}\left[\left(\frac{\nu_{tf}}{\sigma_{kf}} + \nu_f\right)\frac{\partial k_f}{\partial x_j}\right] - \epsilon_f - \frac{18\nu_f}{d^2}\frac{1}{1-C}\left[C\left(2k_f - \overline{u'_{fi} u'_{pi}}\right) + \overline{c' u'_{fi}}\left(U_{fi} - U_{pi}\right)\right] - \frac{18\nu_f}{d^2}\frac{\overline{c' u'_{fi}}}{(1-C)^2}\left[C\left(U_{fi} - U_{pi}\right)\right] \qquad (8)$$

The turbulence energy, its dissipation rate and the production term are defined by

$$k_X = \frac{1}{2}\overline{u'^2_{Xi}} \tag{9}$$

$$\epsilon_X = \nu_X \overline{\frac{u'_{Xi}}{x_j}\frac{u'_{Xi}}{x_j}} \tag{10}$$

$$P_{kX} = -\overline{u'_{Xi}u'_{Xj}}\frac{\partial U_{Xi}}{\partial x_j} \tag{11}$$

where X takes f or p according to the considering phase. The equation of ϵ_f is derived as the same equation as that of the single phase flows when assuming the isotropy of the fine-scale fluctuations (Launder 1975).

In contrast to the usual models, consideration is given to the treatment of the turbulence energy in a solid phase k_p. Its transport equation is derived as follows:

$$\frac{D_p k_p}{Dt} = P_{kp} - \overline{u'_{pj}\frac{\partial}{\partial x_j}\frac{u'^2_{pi}}{2}} + \nu_p \frac{\partial^2 k_p}{\partial x_j^2} - \epsilon_p + \frac{18\nu_f}{d^2}\frac{\rho_f}{\rho_p}\left(\overline{u'_{fi}u'_{pi}} - 2k_p\right) \tag{12}$$

The production term P_{kp} is given by Eq.(11). With the modeling of the second term on the right hand side of Eq.(12), the closed form is given by

$$\frac{D_p k_p}{Dt} = P_{kp} + \frac{\partial}{\partial x_j}\left[\left(\frac{\nu_{tp}}{\sigma_{kp}} + \nu_p\right)\frac{\partial k_p}{\partial x_j}\right] - \epsilon_p + \frac{18\nu_f}{d^2}\frac{\rho_f}{\rho_p}\left(\overline{u'_{fi}u'_{pi}} - 2k_p\right) \tag{13}$$

Furthermore, from Eq.(13), the following algebraic form is derived:

$$k_p = \frac{1}{2}\overline{u'_{fi}u'_{pi}} + \frac{1}{2}\left[\frac{18\nu_f}{d^2}\frac{\rho_f}{\rho_p}\right]^{-1}(P_{kp} - \epsilon_p) \tag{14}$$

Consequently, together with the governing equations for liquid-phase turbulence energy and its dissipation rate, the algebraic equation given by Eq.(14) is solved in the present numerical model.

The Reynolds stress terms included in the governing equations are modeled by the following forms:

$$-\overline{u'_{Xi}u'_{Xj}} = \nu_{tX}\left(\frac{\partial U_{Xi}}{\partial x_j} + \frac{\partial U_{Xj}}{\partial x_i}\right) \quad [X = f \text{ or } p,\ \ i \neq j] \tag{15}$$

The eddy diffusivities ν_{tX} is given by $\nu_{tX} = C_\mu(k_X^2/\epsilon_X)$ where X takes f or p. The turbulent flux $\overline{c'u'_{Xi}}$ is modeled by a gradient-type representation with the turbulent Schmidt number σ_{cX}.

$$-\overline{c'u'_{Xi}} = \frac{\nu_{tX}}{\sigma_{cX}}\frac{\partial C}{\partial x_i} \tag{16}$$

In addition, with the relationships for $\overline{u'_f}$ and $\overline{u'_p}$ (Hosoda and Yogoshi 1987), the turbulence interaction between two phases $\overline{u'_{fi}u'_{pi}}$ is assumed to be given by

$$\overline{u'_{fi}u'_{pi}} = 2k_f\frac{aT_{fL}}{aT_{fL}+1} \tag{17}$$

where $a = 18\rho_f/\rho_p$ and T_{fL} is the Lagrangian time scale for a liquid phase (Calabrese and Middleman 1979), which is given by

$$T_{fL} = \frac{5}{12}\frac{k_f}{\epsilon_f} \tag{18}$$

Finally, taking account of the modeling for the scalar dissipation (Launder 1975), ϵ_p is assumed to be modeled as

$$\epsilon_p = C_{\epsilon p}\frac{\epsilon_f}{k_f}k_p \tag{19}$$

Computational Procedures

The governing equations are discretized in a Lagrangian scheme (Ushijima 1994). The momentum equation for a liquid phase, for example, is written as the following form:

$$U_{fi}^{n+1} = U'^n_{fi} + \left[-PG_i^{n+1} + H_i^n + \left(\frac{3}{2}D'^n_i - \frac{1}{2}D''^{n-1}_i\right)\right]\Delta t \tag{20}$$

where PG_i, H_i and D_i are pressure gradient, external and interactive forces and diffusion terms respectively. In Eq.(20), superscripts stand for the computational step numbers and 'prime' and 'double prime' stand for the variables located on upstream positions at n and $n-1$ time steps respectively.

The first term on the right hand side of Eq.(20), corresponding to a convection term, is evaluated by a local cubic spline interpolation (LCSI) method with third-order accuracy (Ushijima 1994). In a one-dimensional space, as shown in Fig.1, the convected variable ϕ at ξ_m is spatially interpolated between

$\xi_{m_{i-1}}$ and ξ_{m_i} with the following cubic spline function:

$$S_m(\xi_m) = M_{i-1}\frac{(\xi_{m_i}-\xi_m)^3}{6h_i} + M_i\frac{(\xi_m-\xi_{m_{i-1}})^3}{6h_i} + \left(\phi_{i-1} - \frac{M_{i-1}h_i^2}{6}\right)\frac{\xi_{m_i}-\xi_m}{h_i} + \left(\phi_i - \frac{M_i h_i^2}{6}\right)\frac{\xi_m-\xi_{m_{i-1}}}{h_i} \quad (21)$$

where second-order derivatives M_{i-1} and M_i are obtained from the third-order polynomial uniquely determined from the neighboring four values $(\phi_{i-2}, \cdots, \phi_{i+1})$. In a three-dimensional space, the one-dimensional interpolation is repeated in all directions and convected value is evaluated from the surrounding 64 values. This method allows us to have more accurate results than the third-order upwind difference as shown by Ushijima (1994).

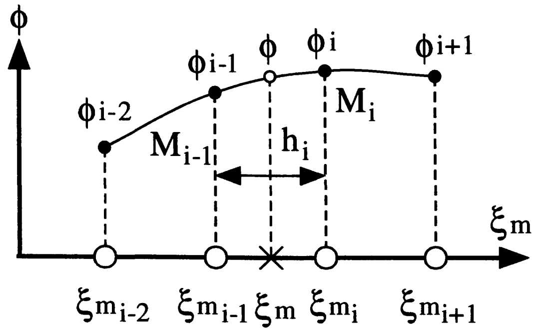

Figure 1: LCSI method in one-dimensional space

Deformation of Bottom Boundary

The bottom boundary profiles are deformed due to the accumulation and resuspension of the particles according to the traction force caused by turbulent flows. The amount of the sand particles p_s lifted up by the turbulent flows is estimated with the following pick-up rate model proposed by Nakagawa and Tsujimoto (1980):

$$p_s\sqrt{\frac{d}{(\rho_p/\rho_f - 1)\,g}} = 0.03\tau_*\left(1 - 0.035/\tau_*\right) \quad (22)$$

where τ_* is the normalized traction force given by

$$\tau_* = \frac{u_*^2}{[(\rho_p/\rho_f - 1)\,gd]} \quad (23)$$

The friction velocity u_* is calculated with horizontal two velocity components, $u_* = (u_{1*}^2 + u_{2*}^2)^{1/2}$, with general logarithmic law for a hydraulically rough wall.

From the calculated p_s, the boundary condition for the average volumetric concentration C is given to the computational cell on the bottom surface. The spatial distributions of C is obtained from the computation of the solid phase governing equations. The amount of the solid particles transported in horizontal directions x_i $(i = 1, 2)$ is estimated from the vertical integration of the flux CU_{pi}. Thus, the level of the bottom surface B can be obtained from the following continuity equation for the bottom materials:

$$(1-\gamma)\frac{\partial B}{\partial t} + \frac{\partial q_i}{\partial x_i} = 0 \quad [i = 1, 2] \quad (24)$$

where γ is the porosity and q_i is the solid phase quantity transported in x_i direction.

The profiles of bottom boundaries are represented with the three dimensional body-fitted coordinates generated by

$$\left(\frac{\partial^2 x_i}{\partial\xi_p\partial\xi_q}\right)^*\left(\frac{\partial\xi_p}{\partial x_j}\right)^*\left(\frac{\partial\xi_q}{\partial x_j}\right)^* + \frac{\partial^2 x_i}{\partial\xi_r\partial\xi_s}\left(\frac{\partial\xi_r}{\partial x_j}\right)^*\left(\frac{\partial\xi_s}{\partial x_j}\right)^* + P_m\left(\frac{\partial x_i}{\partial\xi_m}\right)^* = 0 \quad (25)$$

where P_m is a control function, ξ_m is the coordinates in the transformed space. The asterisk in Eq.(25) means that the derivatives are evaluated with spline functions to increase numerical accuracy (Ushijima 1994).

In accordance with the progress of the boundary deformation, the curvilinear coordinates are regenerated, so that the unsteady deformation of the boundary shapes can be adequately treated. The internal grid points are distributed independently of the fluid velocity, on the basis of the ALE formulation. The effects of the resulting grid velocity are taken into account in the Lagrangian differential operators as indicated in Eq.(7).

The computations for the liquid-solid flows and the deformation of boundary shapes are based on the numerical procedures proposed by Ushijima (1996). Thus, the two processes are calculated alternately with different computational time increments. This method allows us to deal efficiently with two processes having largely different time scales.

APPLICATION TO LIQUID-SOLID FLOWS ON DEFORMED SAND BED

The computational method was applied to the local scouring on a sand bed caused by cooling-water discharge from a power station. Figure 2 shows the geometry and bottom boundary conditions. The bottom surface in front of the outlet structure is covered with concrete blocks and SPAC (Spreading Armor Coat) to prevent the scour. The surrounding area consists of uniform sand particles with the diameter of 0.2mm. The cooling-water is discharged only from the middle outlet with the average velocity of 5.0m/s.

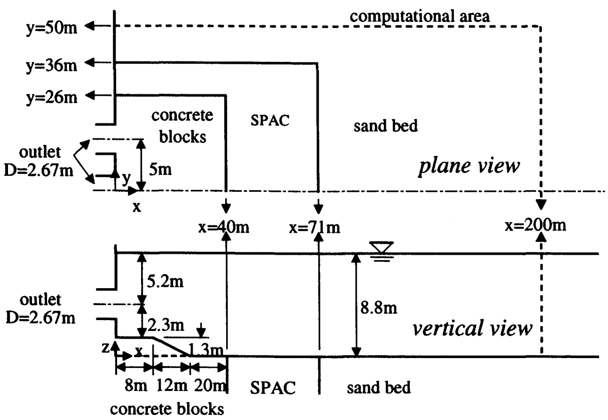

Figure 2: Geometry and boundary conditions

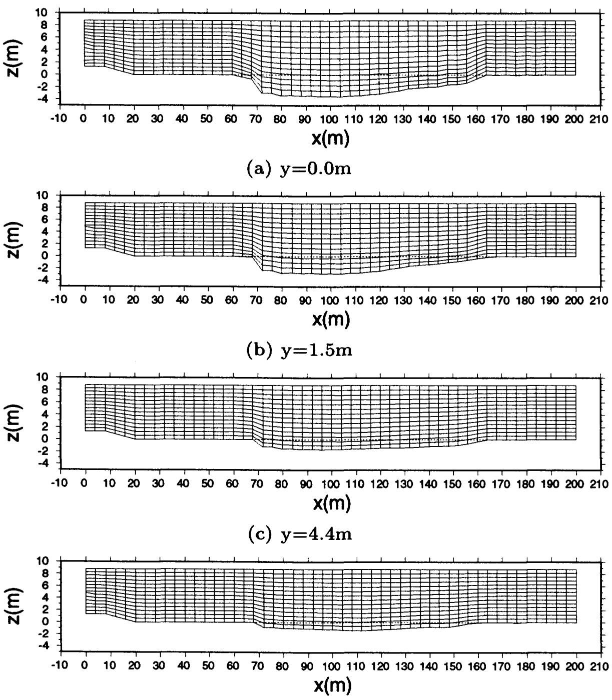

(a) y=0.0m

(b) y=1.5m

(c) y=4.4m

(d) y=7.4m

Figure 3: Generated computational grid

Figures 3 and 4 show the generated curvilinear coordinates and predicted velocity vectors near the symmetrical section when the profiles of bottom boundaries are in the steady state.

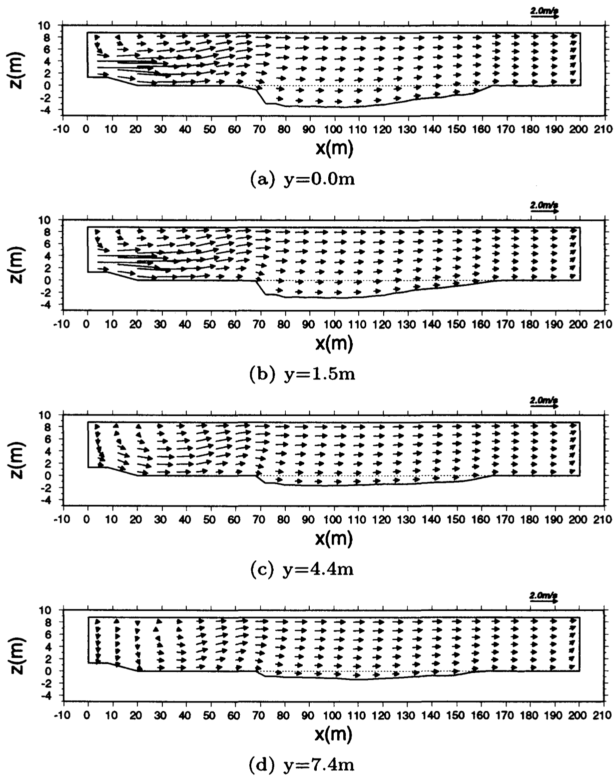

(a) y=0.0m

(b) y=1.5m

(c) y=4.4m

(d) y=7.4m

Figure 4: Predicted velocity vectors in liquid phase

Figure 5 shows the distributions of k_f and k_p/k_f near the outlet. The ratio k_p/k_f ranges from 0.83 to 0.98 in the area of $x = 0$ to $20m$, which indicates that the large turbulence energy of the flow field is transferred to that of the solid phase in this region.

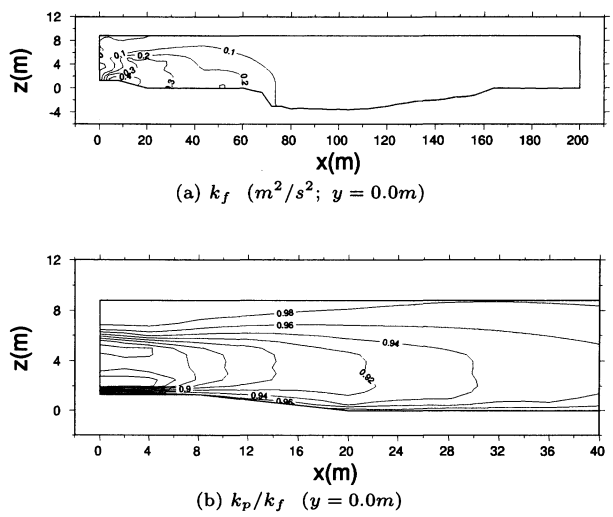

(a) k_f $(m^2/s^2;\ y = 0.0m)$

(b) k_p/k_f $(y = 0.0m)$

Figure 5: Distribution of turbulence energy

Figure 6 shows the predicted velocity vectors in the solid phase. The velocity components in -z direction can be found in this phase due to the density effects.

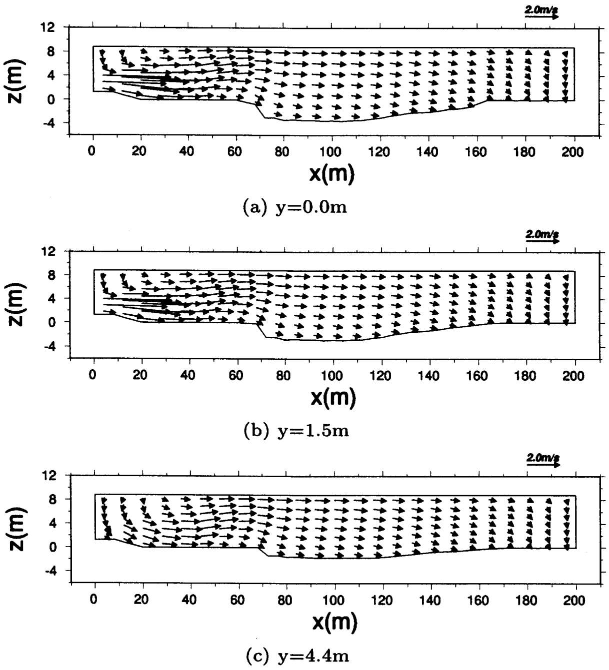

Figure 6: Predicted velocity vectors in solid phase

Finally, Fig. 7 shows the comparison between the field observations and computational results on the sand bed profiles along the center line. This section includes the deeply scoured area. As shown in Fig. 7, the predicted results are in good agreement with the field measurements.

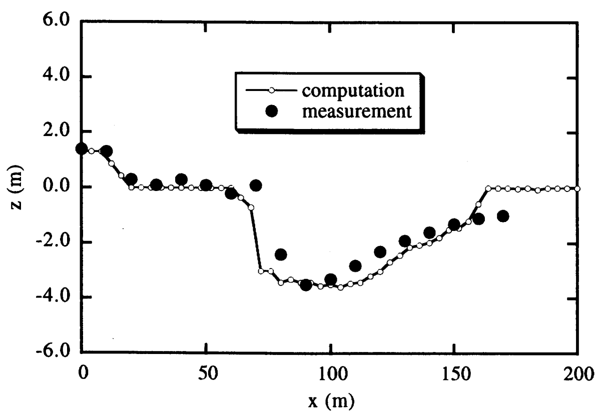

Figure 7: Comparison of sand bed profiles

CONCLUDING REMARKS

A computational method has been developed to predict liquid-solid turbulent flows on moving boundaries with a two-fluid turbulence model. The profiles of the sand bed are represented by regenerating curvilinear coordinates on the basis of the ALE formulation. This computational method was applied to the deformation of the sand bed profiles caused by cooling-water flows. As a result, it was shown that the predicted bed profiles are generally in good agreement with the results obtained by field measurements.

References

Calabrese, R. V. and S. Middleman (1979). The dispersion of discrete particles in a turbulent fluid field. *A.I.Ch.E. 25*, 1025–1035.

Hirt, C. W., A. A. Amsden, and J. L. Cook (1974). An arbitrary Lagrangian-Eulerian computing method for all flow speeds. *Journal of Computational Physics 14*, 227–253.

Hosoda, T. and S. Yogoshi (1987). The basic equations of $k-\epsilon$ model in multi phase flows. *Annual Journal of Hydraulic Engineering, JSCE (in Janapese) 31*, 581–586.

Launder, B. E. (1975). On the effects of a gravitational field on the turbulent transport of heat and momentum. *J. Fluid Mech. 67*, 569–581.

Murray, J. D. (1965). On the mathematics of fluidization part 1. fundamental equations and wave propagation. *J. Fluid Mech. 21*, 465–493.

Nakagawa, H. and T. Tsujimoto (1980). Sand bed instability due to bed load motion. *Proc. ASCE, Journal of Hydraulics Division 106, HY 12*, 2029–2051.

Thompson, J. F., Z. U. A. Warsi, and C. W. Mastin (1985). *Numerical Grid Generation.* Elsevier Science, New York.

Ushijima, S. (1994). Prediction of thermal stratification in a curved duct with 3D boundary-fitted co-ordinates. *International Journal for Numerical Methods in Fluids 19*, 647–665.

Ushijima, S. (1996). Arbitrary Lagrangian-Eulerian numerical prediction for local scour caused by turbulent flows. *Journal of Computational Physics 125*, 71–82.